Available online at www.sciencedirect.com
ScienceDirect
Neurocomputing 71 (2007) 234–243
NEUROCOMPUTING
www.elsevier.com/locate/neucom

Robust intelligent tracking control with PID-type learning algorithm

Chun-Fei Hsu[a,*], Guan-Ming Chen[b], Tsu-Tian Lee[c]

[a]Department of Electrical Engineering, Chung Hua University, Hsinchu 300, Taiwan, ROC
[b]Department of Electrical and Control Engineering, National Chiao-Tung University, Hsinchu 300, Taiwan, ROC
[c]Department of Electrical Engineering, National Taipei University of Technology, Taipei 106, Taiwan, ROC

Received 1 June 2006; received in revised form 22 November 2006; accepted 16 January 2007
Communicated by W. Yu
Available online 14 February 2007

Abstract

This paper proposes a robust intelligent tracking controller (RITC) for a class of unknown nonlinear systems. The proposed RITC system is comprised of a neural controller and a robust controller. The neural controller is designed to approximate an ideal controller using a proportional–integral–derivative (PID)-type learning algorithm in the sense of Lyapunov function, and the robust controller is designed to achieve L^2 tracking performance with desired attenuation level. Finally, to investigate the effectiveness of the RITC system, the proposed design methodology is applied to control two chaotic dynamical systems. The simulation results verify that the proposed RITC system using PID-type learning algorithm can achieve faster convergence of the tracking error and controller parameters than that using I-type learning algorithm.

Keywords: Adaptive control; Neural network control; Robust control; Lyapunov function; Chaotic dynamic system

1. Introduction

Neural networks (NNs) that make use of the organizational principles of human brains are widely known for the powerful abilities, such as learning and adaptation capabilities, fault tolerance, parallelism and generalization. Recently, NN-based control technique has represented an alternative method to solve the control problems [3,4,6,9,10,13]. The most useful property of NNs is their ability to approximate any continuous function to a desired degree of accuracy through learning. Choosing a satisfying tuning algorithm to improve the system performance is the main issue in the NN-based control approaches. Some researchers used the backpropagation method to derive the learning laws; however, it is difficult to guarantee the stability and robustness in the closed-loop system. To tackle this problem, some researchers developed the learning algorithms based on the Lyapunov stability theorem. Although the closed-loop control system stability can be guaranteed, the learning algorithm is in the integral (I)-type form, which should make the convergence of the tracking error and the controller parameters slowly.

Since the number of hidden neurons is not infinite for the real-time practical applications, the approximation errors introduced by the NN approximator cannot be inevitable. In order to ensure the closed-loop control system stability and robustness, a compensation controller will be designed to dispel the approximation error. The most frequently used of compensation controller is like a sliding-mode control, which requires the bound of the approximation error. If the bound of the approximation error is chosen too small, it cannot guarantee the system stabilization in the Lyapunov sense. So, the bound of approximation error is chosen large enough to avoid instability in the practical applications. It can be seen that a large bound of approximation error will result in substantial chattering of the control effort. The chattering phenomena in control efforts will wear the bearing mechanism and excite unmodelled dynamics. To tackle this problem, an error estimation mechanism is investigated to estimate the bound of approximation error so that the chattering phenomenon of the control effort can be reduced [7,12]. However, the adaptive law for the estimation error bound will make it go to infinity.

*Corresponding author.
E-mail addresses: fei@chu.edu.tw (C.-F. Hsu), u9212810@cn.nctu.edu.tw (G.-M. Chen), ttlee@ntut.edu.tw (T.-T. Lee).

0925-2312/$ - see front matter © 2007 Elsevier B.V. All rights reserved.
doi:10.1016/j.neucom.2007.01.002

In the past decade, robust control techniques have been applied extensively in the efficient treatment of robust stabilization and disturbance rejection problems. The L^2-norm has been widely used as a measure of the robustness for a given feedback control system. It has been shown that the L^2-norm bound (desired L^2 performance) can be achieved if an associated Hamilton–Jacobi inequality admits a positive-definite solution. The smaller L^2-norm means the larger degree of robustness. Combing the robust control with NN-based control, some robust NN-based control approaches have been proposed to attenuate the effects of approximation error to a prescribed level [1,15].

In this paper, a robust intelligent tracking controller (RITC), which combines adaptive control, NN control and robust control techniques, is proposed for a class of unknown nonlinear systems. All the controller parameters are online tuned based on the Lyapunov function to achieve favorable approximation performance. A proportional–integral–derivative (PID)-type learning algorithm is used to speed up the convergence of the tracking error and the controller parameters. By the L^2 control design technique, the approximation error can be attenuated to arbitrary specified level. Simulation results are performed to demonstrate the effectiveness of the proposed RITC design method. The major contributions of this paper are: (1) the successful development of an RITC system via L^2 tracking performance is used to compensate the residual of the approximation error; (2) the convergence of the tracking error and control parameter is accelerated by the PID-type learning algorithm, and (3) the successful application of the RITC to control two chaotic dynamic systems.

2. Description of neural network approximator

A general function of a three-layer NN as shown in Fig. 1 can be represented in the following form [4]:

$$y = \sum_{j=1}^{m} w_j \xi_j(z_i, v_{ij}, c_j, s_j), \tag{1}$$

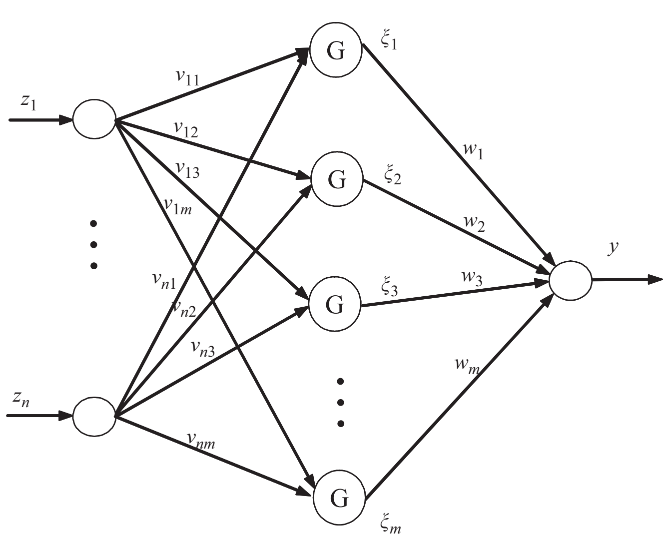

Fig. 1. The structure of neural network.

where $z = [z_1 z_2 \dots z_n]^{\mathrm{T}}$ and y are the input and output variables, respectively; ξ_j represents the active function of the jth neuron in the hidden layer; v_{ij} denotes the weight between the input layer and hidden layer; w_j denotes the weight between the hidden layer and output layer; and c_i and s_i are the center and width of the jth active function, respectively. The active function of the jth hidden neuron can be represented as

$$\xi_j = \exp\left(-\frac{\left(\Sigma_{i=1}^{n} z_i v_{ij} - c_j\right)^2}{s_j^2}\right). \tag{2}$$

Define the vectors **c**, **s** and **v** collecting all parameters of the hidden layer as

$$\mathbf{c} = [c_1 c_2 \dots c_m]^{\mathrm{T}}, \tag{3}$$

$$\mathbf{s} = [s_1 s_2 \dots s_m]^{\mathrm{T}}, \tag{4}$$

$$\mathbf{v} = [v_1 v_2 \dots v_m], \tag{5}$$

in which $\mathbf{v}_i = [v_{1i} \dots v_{ni}]^{\mathrm{T}}$. Then, the output of the NN can be represented in a vector form

$$y = \mathbf{w}^{\mathrm{T}} \boldsymbol{\xi}(\mathbf{v}^{\mathrm{T}}\mathbf{z}, \mathbf{c}, \mathbf{s}), \tag{6}$$

where $\mathbf{w} = [w_1 w_2 \dots w_m]^{\mathrm{T}}$ and $\boldsymbol{\xi} = [\xi_1 \xi_2 \dots \xi_m]^{\mathrm{T}}$.

The main property of NN regarding feedback control purpose is the universal function approximation property. It implies that there exists an expansion of (6) such that it can uniformly approximate a nonlinear even time-varying function Θ. By the universal approximation theorem, there exists an optimal NN approximator y^* such that [14]

$$\Theta = y^* + \Delta = \mathbf{w}^{*\mathrm{T}} \boldsymbol{\xi}^*(\mathbf{v}^{*\mathrm{T}}\mathbf{z}, \mathbf{c}^*, \mathbf{s}^*) + \Delta, \tag{7}$$

where $\mathbf{w}^*$ and $\boldsymbol{\xi}^*$ are the optimal vectors of **w** and $\boldsymbol{\xi}$, respectively; $\mathbf{c}^*$, $\mathbf{s}^*$ and $\mathbf{v}^*$ are the optimal vectors of **c**, **s** and **v**, respectively; and Δ denotes the approximation error. In fact, the optimal vector that is needed to best approximate a nonlinear function is difficult to determine and even might not be unique. Thus, a NN estimator is defined as

$$\hat{y} = \hat{\mathbf{w}}^{\mathrm{T}} \hat{\boldsymbol{\xi}}(\hat{\mathbf{v}}^{\mathrm{T}}\mathbf{z}, \hat{\mathbf{c}}, \hat{\mathbf{s}}), \tag{8}$$

where $\hat{\mathbf{w}}$ and $\hat{\boldsymbol{\xi}}$ are the estimation vector of $\mathbf{w}^*$ and $\boldsymbol{\xi}^*$, respectively; $\hat{\mathbf{c}}$, $\hat{\mathbf{s}}$ and $\hat{\mathbf{v}}$ are the estimation vectors of $\mathbf{c}^*$, $\mathbf{s}^*$ and $\mathbf{v}^*$, respectively. The approximation error is denoted as

$$\tilde{y} = \Theta - \hat{y} = \mathbf{w}^{*\mathrm{T}} \boldsymbol{\xi}^* - \hat{\mathbf{w}}^{\mathrm{T}} \hat{\boldsymbol{\xi}} + \Delta = \tilde{\mathbf{w}}^{\mathrm{T}} \hat{\boldsymbol{\xi}} + \hat{\mathbf{w}}^{\mathrm{T}} \tilde{\boldsymbol{\xi}} + \tilde{\mathbf{w}}^{\mathrm{T}} \tilde{\boldsymbol{\xi}} + \Delta, \tag{9}$$

where $\tilde{\mathbf{w}} = \mathbf{w}^* - \hat{\mathbf{w}}$ and $\tilde{\boldsymbol{\xi}} = \boldsymbol{\xi}^* - \hat{\boldsymbol{\xi}}$. In the following, some adaptive laws will be proposed to online tune the parameters of the NN estimator to achieve favorable approximation performance. To achieve this goal, the Taylor linearization technique is employed to transform the nonlinear active function into partially linear form so that the expansion can be expressed as [4]

$$\tilde{\boldsymbol{\xi}} = \begin{bmatrix} \tilde{\xi}_1 \\ \tilde{\xi}_2 \\ \vdots \\ \tilde{\xi}_m \end{bmatrix} = \begin{bmatrix} \frac{\partial \xi_1}{\partial(\mathbf{v}^{\mathrm{T}}\mathbf{z})} \\ \frac{\partial \xi_2}{\partial(\mathbf{v}^{\mathrm{T}}\mathbf{z})} \\ \vdots \\ \frac{\partial \xi_m}{\partial(\mathbf{v}^{\mathrm{T}}\mathbf{z})} \end{bmatrix}\Bigg|_{\mathbf{v}^{\mathrm{T}}\mathbf{z}=\hat{\mathbf{v}}^{\mathrm{T}}\mathbf{z}} (\mathbf{v}^{*\mathrm{T}}\mathbf{z} - \hat{\mathbf{v}}^{\mathrm{T}}\mathbf{z}) + \begin{bmatrix} \frac{\partial \xi_1}{\partial \mathbf{c}} \\ \frac{\partial \xi_2}{\partial \mathbf{c}} \\ \vdots \\ \frac{\partial \xi_m}{\partial \mathbf{c}} \end{bmatrix}\Bigg|_{\mathbf{c}=\hat{\mathbf{c}}} (\mathbf{c}^* - \hat{\mathbf{c}}) + \begin{bmatrix} \frac{\partial \xi_1}{\partial \mathbf{s}} \\ \frac{\partial \xi_2}{\partial \mathbf{s}} \\ \vdots \\ \frac{\partial \xi_m}{\partial \mathbf{s}} \end{bmatrix}\Bigg|_{\mathbf{s}=\hat{\mathbf{s}}} (\mathbf{s}^* - \hat{\mathbf{s}}) + \mathbf{h}, \tag{10}$$

or

$$\tilde{\boldsymbol{\xi}} = \boldsymbol{\xi}_{\mathbf{v}}^{\mathrm{T}}\tilde{\mathbf{v}}^{\mathrm{T}}\mathbf{z} + \boldsymbol{\xi}_{\mathbf{c}}^{\mathrm{T}}\tilde{\mathbf{c}} + \boldsymbol{\xi}_{\mathbf{s}}^{\mathrm{T}}\tilde{\mathbf{s}} + \mathbf{h}, \tag{11}$$

where $\mathbf{h}$ represents the higher-order term; $\tilde{\mathbf{v}} = \mathbf{v}^* - \hat{\mathbf{v}}$; $\tilde{\mathbf{c}} = \mathbf{c}^* - \hat{\mathbf{c}}$; $\tilde{\mathbf{s}} = \mathbf{s}^* - \hat{\mathbf{s}}$ and

$$\boldsymbol{\xi}_{\mathbf{v}} = \left[\frac{\partial \xi_1}{\partial(\mathbf{v}^{\mathrm{T}}\mathbf{z})} \quad \frac{\partial \xi_2}{\partial(\mathbf{v}^{\mathrm{T}}\mathbf{z})} \quad \cdots \quad \frac{\partial \xi_m}{\partial(\mathbf{v}^{\mathrm{T}}\mathbf{z})}\right]\Bigg|_{\mathbf{v}^{\mathrm{T}}\mathbf{z}=\hat{\mathbf{v}}^{\mathrm{T}}\mathbf{z}}, \tag{12}$$

$$\boldsymbol{\xi}_{\mathbf{c}} = \left[\frac{\partial \xi_1}{\partial \mathbf{c}} \quad \frac{\partial \xi_2}{\partial \mathbf{c}} \quad \cdots \quad \frac{\partial \xi_m}{\partial \mathrm{c}}\right]\Bigg|_{\mathbf{c}=\hat{\mathbf{c}}}, \tag{13}$$

$$\boldsymbol{\xi}_{\mathbf{s}} = \left[\frac{\partial \xi_1}{\partial s} \quad \frac{\partial \xi_2}{\partial s} \quad \cdots \quad \frac{\partial \xi_m}{\partial \mathbf{s}}\right]\Bigg|_{\mathbf{s}=\hat{\mathbf{s}}}. \tag{14}$$

Substituting (11) into (9), it is obtained that

$$\tilde{y} = \tilde{\mathbf{w}}^{\mathrm{T}}\hat{\boldsymbol{\xi}} + \hat{\mathbf{w}}^{\mathrm{T}}\boldsymbol{\xi}_{\mathbf{v}}^{\mathrm{T}}\tilde{\mathbf{v}}^{\mathrm{T}}z + \hat{\mathbf{w}}^{\mathrm{T}}\boldsymbol{\xi}_{\mathbf{c}}^{\mathrm{T}}\tilde{\mathbf{c}} + \hat{\mathbf{w}}^{\mathrm{T}}\boldsymbol{\xi}_{\mathbf{s}}^{\mathrm{T}}\tilde{\mathbf{s}} + \varepsilon_1, \tag{15}$$

where $\varepsilon_1 = \hat{\mathbf{w}}^{\mathrm{T}}\mathbf{h} + \tilde{\mathbf{w}}^{\mathrm{T}}\tilde{\boldsymbol{\xi}} + \Delta$. To speed up the convergence of NN learning, the optimal vector $\mathbf{w}^*$ is decomposed into three parts as

$$\mathbf{w}^* = \beta_{\mathrm{P}}\boldsymbol{\Omega}_{\mathrm{P}}^* + \beta_{\mathrm{I}}\boldsymbol{\Omega}_{\mathrm{I}}^* + \beta_{\mathrm{D}}\boldsymbol{\Omega}_{\mathrm{D}}^*, \tag{16}$$

where $\boldsymbol{\Omega}_{\mathrm{P}}^*$, $\boldsymbol{\Omega}_{\mathrm{I}}^*$ and $\boldsymbol{\Omega}_{\mathrm{D}}^*$ are the proportional, integral and derivative terms of $\mathbf{w}^*$, respectively; β_{P}, β_{I}, and β_{D} are positive constants; $\boldsymbol{\Omega}_{\mathrm{I}}^* = \int \boldsymbol{\Omega}_{\mathrm{P}}^* \,\mathrm{d}\tau$ and $\boldsymbol{\Omega}_{\mathrm{D}}^* = \mathrm{d}\boldsymbol{\Omega}_{\mathrm{P}}^*/\mathrm{d}t$. The estimation vector $\hat{\mathbf{w}}$ is given as

$$\hat{\mathbf{w}} = \beta_{\mathrm{P}}\hat{\boldsymbol{\Omega}}_{\mathrm{P}} + \beta_{\mathrm{I}}\hat{\boldsymbol{\Omega}}_{\mathrm{I}} + \beta_{\mathrm{D}}\hat{\boldsymbol{\Omega}}_{\mathrm{D}}, \tag{17}$$

where $\hat{\boldsymbol{\Omega}}_{\mathrm{P}}$, $\hat{\boldsymbol{\Omega}}_{\mathrm{I}}$ and $\hat{\boldsymbol{\Omega}}_{\mathrm{D}}$ are the proportional, integral and derivative terms of $\hat{\mathbf{w}}$, respectively; $\hat{\boldsymbol{\Omega}}_{\mathrm{I}} = \int \hat{\boldsymbol{\Omega}}_{\mathrm{P}} \,\mathrm{d}\tau$ and $\hat{\boldsymbol{\Omega}}_{\mathrm{D}} = \mathrm{d}(\hat{\boldsymbol{\Omega}}_{\mathrm{P}}/\mathrm{d}t)$. Thus, $\tilde{\mathbf{w}}$ can be expressed as

$$\tilde{\mathbf{w}} = \beta_{\mathrm{I}}\tilde{\boldsymbol{\Omega}}_{\mathrm{I}} - \beta_{\mathrm{P}}\hat{\boldsymbol{\Omega}}_{\mathrm{P}} - \beta_{\mathrm{D}}\hat{\boldsymbol{\Omega}}_{\mathrm{D}} + \varepsilon_2, \tag{18}$$

where $\tilde{\boldsymbol{\Omega}}_{\mathrm{I}} = \boldsymbol{\Omega}_{\mathrm{I}}^* - \hat{\boldsymbol{\Omega}}_{\mathrm{I}}$ and $\varepsilon_2 = \beta_{\mathrm{P}}\boldsymbol{\Omega}_{\mathrm{P}}^* + \beta_{\mathrm{D}}\boldsymbol{\Omega}_{\mathrm{D}}^*$. Substituting (18) into (15), we obtain that

$$\begin{aligned} \tilde{y} &= \beta_{\mathrm{I}}\tilde{\boldsymbol{\Omega}}_{\mathrm{I}}^{\mathrm{T}}\hat{\boldsymbol{\xi}} - \beta_{\mathrm{P}}\hat{\boldsymbol{\Omega}}_{\mathrm{P}}^{\mathrm{T}}\hat{\boldsymbol{\xi}} - \beta_{\mathrm{D}}\hat{\boldsymbol{\Omega}}_{\mathrm{D}}^{\mathrm{T}}\hat{\boldsymbol{\xi}} + \hat{\mathbf{w}}^{\mathrm{T}}\boldsymbol{\xi}_{\mathbf{v}}^{\mathrm{T}}\tilde{\mathbf{v}}^{\mathrm{T}}\mathbf{z} \\ &\quad + \hat{\mathbf{w}}^{\mathrm{T}}\boldsymbol{\xi}_{\mathbf{c}}^{\mathrm{T}}\tilde{\mathbf{c}} + \hat{\mathbf{w}}^{\mathrm{T}}\boldsymbol{\xi}_{\mathbf{s}}^{\mathrm{T}}\tilde{\mathbf{s}} + \varepsilon \\ &= \beta_{\mathrm{I}}\tilde{\boldsymbol{\Omega}}_{\mathrm{I}}^{\mathrm{T}}\hat{\boldsymbol{\xi}} - \beta_{\mathrm{P}}\hat{\boldsymbol{\Omega}}_{\mathrm{P}}^{\mathrm{T}}\hat{\boldsymbol{\xi}} - \beta_{\mathrm{D}}\hat{\boldsymbol{\Omega}}_{\mathrm{D}}^{\mathrm{T}}\hat{\boldsymbol{\xi}} + \hat{\mathbf{w}}^{\mathrm{T}}\boldsymbol{\xi}_{\mathbf{v}}^{\mathrm{T}}\tilde{\mathbf{v}}^{\mathrm{T}}\mathbf{z} \\ &\quad + \tilde{\mathbf{c}}^{\mathrm{T}}\boldsymbol{\xi}_{\mathbf{c}}\hat{\mathbf{w}} + \tilde{\mathbf{s}}^{\mathrm{T}}\boldsymbol{\xi}_{\mathbf{s}}\hat{\mathbf{w}} + \varepsilon, \end{aligned} \tag{19}$$

where $\hat{\mathbf{w}}^{\mathrm{T}}\boldsymbol{\xi}_{\mathbf{c}}^{\mathrm{T}}\tilde{\mathbf{c}} = \tilde{\mathbf{c}}^{\mathrm{T}}\boldsymbol{\xi}_{\mathbf{c}}\hat{\mathbf{w}}$ and $\hat{\mathbf{w}}^{\mathrm{T}}\boldsymbol{\xi}_{\mathbf{s}}^{\mathrm{T}}\tilde{\mathbf{s}} = \tilde{\mathbf{s}}^{\mathrm{T}}\boldsymbol{\xi}_{\mathbf{s}}\hat{\mathbf{w}}$ since they are scalars, and the uncertain term $\varepsilon = \varepsilon_2^{\mathrm{T}}\hat{\boldsymbol{\xi}} + \varepsilon_1$.

3. Design of robust intelligent tracking controller

3.1. Description of ideal control

Consider an nth-order nonlinear system of the controllable canonical form

$$x^{(n)} = F(\mathbf{x}) + G(\mathbf{x})u, \tag{20}$$

where $\mathbf{x} = [x\dot{x}\ldots x^{(n-1)}]^{\mathrm{T}}$ is the state vector of the system, which is assumed to be available for measurement, $\mathrm{F}(\mathbf{x})$ and $\mathrm{G}(\mathbf{x})$ are the nonlinear system dynamics which can be unknown, and u is the input of the system. Since the nonlinear dynamics cannot be exactly obtained, the considered system poses an interesting and challenging dilemma to the control problem. Assume that the system dynamics in the controlled system (20) are exactly known. The nominal model of (20) can be represented as

$$x^{(n)} = f_n(\mathbf{x}) + g_n(\mathbf{x})u, \tag{21}$$

where $\mathrm{f_n}(\mathbf{x})$ and is the nominal value of $\mathrm{F}(\mathbf{x})$, and $\mathrm{g_n}(\mathbf{x}) > 0$ is a nominal constant of $\mathrm{G}(\mathbf{x})$. In the presence of uncertainties, the considered system (20) can be described as

$$\begin{aligned} x^{(n)} &= [f_n(\mathbf{x}) + \Delta f(\mathbf{x})] + [g_n(\mathbf{x}) + \Delta g(\mathbf{x})]u \\ &= f(\mathbf{x}) + g_n(\mathbf{x})u, \end{aligned} \tag{22}$$

where $\Delta\mathrm{f}(\mathbf{x})$ and $\Delta\mathrm{g}(\mathbf{x})$ denote the uncertainties; $\mathrm{f}(\mathbf{x})$ is defined as $f(\mathbf{x}) \equiv f_n(\mathbf{x}) + \Delta f(\mathbf{x}) + \Delta g_n(\mathbf{x})u$.

The tracking control problem of the system is to find a control law so that the state trajectory x can track a reference command x_{c} closely. The tracking error is defined as

$$e = x_{\mathrm{c}} - x. \tag{23}$$

There exits an ideal controller defined as [11]

$$u^* = \frac{1}{g_n(\mathbf{x})}[-f(\mathbf{x}) + x_{\mathrm{c}}^{(n)} + \mathbf{k}^{\mathrm{T}}\mathbf{e}], \tag{24}$$

where $\mathbf{e} = [e\dot{e}\ldots e^{(n-1)}]^{\mathrm{T}}$ is the tracking error vector and $\mathbf{k} = [k_n \ldots k_2 k_1]^{\mathrm{T}}$, in which $\mathrm{k_i}$, $i = 1, 2, \ldots, n$ are positive constants. Applying the ideal controller (24) to system (22) results in the following error dynamics

$$e^{(n)} + k_1 e^{(n-1)} + \cdots k_n e = 0. \tag{25}$$

If $\mathrm{k_i}$ are chosen such that all roots of the polynomial $h(s) \underline{\underline{\Delta}}\, s^n + k_1 s^{n-1} + \cdots k_n$ lie strictly in the open left half of the complex plane, then it implies that $\lim_{t\to\infty} e = 0$ for any starting initial conditions. However, since the system dynamics $f(\mathbf{x})$ may be unknown or perturbed in practical applications, the ideal controller (24) cannot be precisely obtained. So a model-free design method termed as the RITC will be developed for the unknown nonlinear systems.

3.2. Design of RITC

For achieving a favorable tracking performance and an arbitrarily small attenuation level simultaneously, the developed RITC system shown in Fig. 2 is assumed to take the following form

$$u_{rt} = u_{nc} + u_{rc}, \tag{26}$$

where u_{nc} is the neural controller and u_{rc} is the robust controller. The neural controller is the principal controller, which uses a NN to approximate the ideal controller in (24). The input of the NN is the tracking vector, and the output of the NN is the neural controller, which uses a NN to approximate the ideal controller. The robust controller is designed to achieve a specified L^2 robust tracking performance. Substituting (26) into (22) and using (24) yields

$$\dot{\mathbf{e}} = \mathbf{A}\mathbf{e} + g_n\mathbf{b}(u^* - u_{nc} - u_{rc}), \tag{27}$$

where

$$\mathbf{A} = \begin{bmatrix} 0 & 1 & 0 & \cdots & 0 \\ \vdots & \ddots & \ddots & \ddots & 0 \\ 0 & \cdots & \cdots & 0 & 1 \\ -k_n & -k_{n-1} & \cdots & \cdots & -k_1 \end{bmatrix}$$

and $\mathbf{b} = [00\ldots1]^T$. By the approximation theorem of the NN (19), (27) can be rewritten as

$$\dot{\mathbf{e}} = \mathbf{A}\mathbf{e} + g_n\mathbf{b}(\beta_I\tilde{\mathbf{\Omega}}_I^T\hat{\boldsymbol{\xi}} - \beta_P\hat{\mathbf{\Omega}}_P^T\hat{\boldsymbol{\xi}} - \beta_D\hat{\mathbf{\Omega}}_D^T\hat{\boldsymbol{\xi}} + \hat{\mathbf{w}}^T\boldsymbol{\xi}_v^T\tilde{\mathbf{v}}^T\mathbf{e} + \tilde{\mathbf{c}}^T\boldsymbol{\xi}_c\hat{\mathbf{w}} + \tilde{\mathbf{s}}^T\boldsymbol{\xi}_s\hat{\mathbf{w}} + \varepsilon - u_{rc}). \tag{28}$$

In the following theorem, we show how to determine the control law, ensuring the stability and robustness of the closed-loop system.

Theorem. *Consider a SISO nonlinear system represented by* (22) *and the control system is designed as* (26). *The neural controller is given as* $u_{nc} = \hat{\mathbf{w}}^T\hat{\boldsymbol{\xi}}(\hat{\mathbf{v}}^T\mathbf{e}, \hat{\mathbf{c}}, \hat{\mathbf{s}})$, *in which* $\hat{\mathbf{w}} = \beta_P\hat{\mathbf{\Omega}}_P + \beta_I\hat{\mathbf{\Omega}}_I + \beta_D\hat{\mathbf{\Omega}}_D$, *with*

$$\hat{\mathbf{\Omega}}_P = \mathbf{e}^T\mathbf{P}\mathbf{b}\hat{\boldsymbol{\xi}}, \tag{29}$$

$$\hat{\mathbf{\Omega}}_I = \int_0^t \mathbf{e}^T\mathbf{P}\mathbf{b}\hat{\boldsymbol{\xi}}\,dt, \tag{30}$$

$$\hat{\mathbf{\Omega}}_D = \frac{d}{dt}(\mathbf{e}^T\mathbf{P}\mathbf{b}\hat{\boldsymbol{\xi}}) \tag{31}$$

and the adaptive laws are designed as

$$\dot{\tilde{\mathbf{v}}} = -\dot{\hat{\mathbf{v}}} = \beta_v\mathbf{e}^T\mathbf{P}\mathbf{b}\mathbf{e}\hat{\mathbf{w}}^T\boldsymbol{\xi}_v, \tag{32}$$

$$\dot{\tilde{\mathbf{c}}} = -\dot{\hat{\mathbf{c}}} = \beta_c\mathbf{e}^T\mathbf{P}\mathbf{b}\boldsymbol{\xi}_c\hat{\mathbf{w}}, \tag{33}$$

$$\dot{\tilde{\mathbf{s}}} = -\dot{\hat{\mathbf{s}}} = \beta_s\mathbf{e}^T\mathbf{P}\mathbf{b}\boldsymbol{\xi}_s\hat{\mathbf{w}}, \tag{34}$$

where learning rates β_v, β_c, *and* β_s *are positive constants. The robust controller is given as*

$$u_{rc} = \frac{1}{2g_n\delta}\mathbf{b}^T\mathbf{P}\mathbf{e}, \tag{35}$$

where the symmetric positive definite matrix $\mathbf{P}$ *satisfies the following Riccati-like equation*

$$\mathbf{A}^T\mathbf{P} + \mathbf{P}\mathbf{A} + \mathbf{Q} + \mathbf{P}\mathbf{b}\left(\frac{1}{\rho^2} - \frac{1}{\delta}\right)\mathbf{b}^T\mathbf{P} = 0, \tag{36}$$

where $\mathbf{Q}$ *is a symmetric positive matrix and* $\rho^2 > \delta$. *Then the RITC system can guarantee the global stability and robustness of the closed-loop system and achieve the following* L^2 *criterion*

$$\int_0^t \mathbf{e}^T\mathbf{e}\,dt \leqslant \frac{2}{\lambda_{\min}(\mathbf{Q})}V(0) + \frac{g_n^2\rho^2}{\lambda_{\min}(\mathbf{Q})}\int_0^t \varepsilon^2\,dt, \tag{37}$$

where $\lambda_{\min}(\mathbf{Q})$ *is the minimal eigenvalue of* $\mathbf{Q}$.

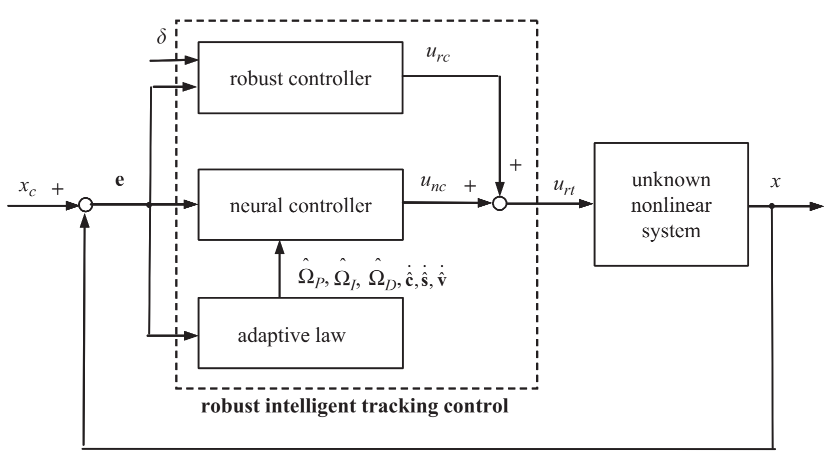

Fig. 2. RITC for unknown nonlinear system.

Proof. Define the Lyapunov function candidate as

$$V = \frac{1}{2}\mathbf{e}^{\mathrm{T}}\mathbf{P}\mathbf{e} + \frac{g_n}{2\beta_v}\mathrm{tr}\{\tilde{v}^{\mathrm{T}}\tilde{v}\} + \frac{g_n}{2\beta_c}\tilde{\mathbf{c}}^{\mathrm{T}}\tilde{\mathbf{c}} + \frac{g_n}{2\beta_s}\tilde{\mathbf{s}}^{\mathrm{T}}\tilde{\mathbf{s}} + \frac{g_n\beta_{\mathrm{D}}}{2}\hat{\mathbf{\Omega}}_{\mathrm{P}}^{\mathrm{T}}\hat{\mathbf{\Omega}}_{\mathrm{P}} + \frac{g_n\beta_{\mathrm{I}}}{2}\tilde{\mathbf{\Omega}}_{\mathrm{I}}^{\mathrm{T}}\tilde{\mathbf{\Omega}}_{\mathrm{I}}. \tag{38}$$

Differentiating (38) with respect to time and using (28) yields

$$\begin{aligned}\dot{V} &= \frac{1}{2}\mathbf{e}^{\mathrm{T}}\mathbf{P}\dot{\mathbf{e}} + \frac{1}{2}\dot{\mathbf{e}}^{\mathrm{T}}\mathbf{P}\mathbf{e} + \frac{g_n}{\beta_v}\mathrm{tr}\{\tilde{\mathbf{v}}^{\mathrm{T}}\dot{\tilde{\mathbf{v}}}\} + \frac{g_n}{\beta_c}\tilde{\mathbf{c}}^{\mathrm{T}}\dot{\tilde{\mathbf{c}}} \\ &\quad + \frac{g_n}{\beta_{\mathbf{s}}}\tilde{\mathbf{s}}^{\mathrm{T}}\dot{\tilde{\mathbf{s}}} + g_n\beta_{\mathrm{D}}\hat{\mathbf{\Omega}}_{\mathrm{P}}^{\mathrm{T}}\dot{\hat{\mathbf{\Omega}}}_{\mathrm{P}} + g_n\beta_{\mathrm{I}}\tilde{\mathbf{\Omega}}_{\mathrm{I}}^{\mathrm{T}}\dot{\tilde{\mathbf{\Omega}}}_{\mathrm{I}} \\ &= \frac{1}{2}\mathbf{e}^{\mathrm{T}}(\mathbf{A}^{\mathrm{T}}\mathbf{P} + \mathbf{P}\mathbf{A})\mathbf{e} + g_n\mathbf{e}^{\mathrm{T}}\mathbf{P}\mathbf{b}(\beta_{\mathrm{I}}\tilde{\mathbf{\Omega}}_{\mathrm{I}}^{\mathrm{T}}\hat{\boldsymbol{\xi}} \\ &\quad - \beta_{\mathrm{P}}\hat{\mathbf{\Omega}}_{\mathrm{P}}^{\mathrm{T}}\hat{\boldsymbol{\xi}} - \beta_{\mathrm{D}}\hat{\mathbf{\Omega}}_{\mathrm{D}}^{\mathrm{T}}\hat{\boldsymbol{\xi}} + \hat{\mathbf{w}}^{\mathrm{T}}\xi_{\mathbf{v}}^{\mathrm{T}}\tilde{\mathbf{v}}^{\mathrm{T}}\mathbf{e} + \tilde{\mathbf{c}}^{\mathrm{T}}\xi_{\mathbf{c}}\hat{\mathbf{w}} \\ &\quad + \tilde{\mathbf{s}}^{\mathrm{T}}\boldsymbol{\xi}_{\mathbf{s}}\hat{\mathbf{w}} + \varepsilon - u_{\mathrm{rc}}) + \frac{g_n}{\beta_v}\mathrm{tr}\{\tilde{\mathbf{v}}^{\mathrm{T}}\dot{\tilde{\mathbf{v}}}\} \\ &\quad + \frac{g_n}{\beta_c}\tilde{\mathbf{c}}^{\mathrm{T}}\dot{\tilde{\mathbf{c}}} + \frac{g_n}{\beta_s}\tilde{\mathbf{s}}^{\mathrm{T}}\dot{\tilde{\mathbf{s}}} + g_n\beta_{\mathrm{D}}\hat{\mathbf{\Omega}}_{\mathrm{P}}^{\mathrm{T}}\dot{\hat{\mathbf{\Omega}}}_{\mathrm{P}} + g_n\beta_{\mathrm{I}}\tilde{\mathbf{\Omega}}_{\mathrm{I}}^{\mathrm{T}}\dot{\tilde{\mathbf{\Omega}}}_{\mathrm{I}} \\ &= \frac{1}{2}e^{\mathrm{T}}(\mathbf{A}^{\mathrm{T}}\mathbf{P} + \mathbf{P}\mathbf{A})\mathbf{e} + g_n\mathbf{e}^{\mathrm{T}}\mathbf{P}\mathbf{b}(-\beta_{\mathrm{P}}\hat{\mathbf{\Omega}}_{\mathrm{P}}^{\mathrm{T}}\hat{\boldsymbol{\xi}} \\ &\quad - \beta_{\mathrm{D}}\hat{\mathbf{\Omega}}_{\mathrm{D}}^{\mathrm{T}}\hat{\boldsymbol{\xi}} + \varepsilon - u_{\mathrm{rc}}) + g_n\beta_{\mathrm{I}}\tilde{\mathbf{\Omega}}_{\mathrm{I}}^{\mathrm{T}}(\mathbf{e}^{\mathrm{T}}\mathbf{P}\mathbf{b}\hat{\boldsymbol{\xi}} + \dot{\tilde{\mathbf{\Omega}}}_{\mathrm{I}}) \\ &\quad + \mathrm{tr}\left\{g_n\tilde{\mathbf{v}}^{\mathrm{T}}\left(\mathbf{e}^{\mathrm{T}}\mathbf{P}\mathbf{b}\mathbf{e}\hat{\mathbf{w}}^{\mathrm{T}}\xi_{\mathbf{v}} + \frac{\dot{\tilde{\mathbf{v}}}}{\beta_v}\right)\right\} \\ &\quad + g_n\tilde{\mathbf{c}}^{\mathrm{T}}\left(\mathbf{e}^{\mathrm{T}}\mathbf{P}\mathbf{b}\xi_{\mathbf{c}}\hat{\mathbf{w}} + \frac{\dot{\tilde{\mathbf{c}}}}{\beta_c}\right) \\ &\quad + g_n\tilde{\mathbf{s}}^{\mathrm{T}}\left(\mathbf{e}^{\mathrm{T}}\mathbf{P}\mathbf{b}\xi_{\mathbf{s}}\hat{\mathbf{w}} + \frac{\dot{\tilde{\mathbf{s}}}}{\beta_{\mathbf{s}}}\right) + g_n\beta_{\mathrm{D}}\hat{\mathbf{\Omega}}_{\mathrm{P}}^{\mathrm{T}}\dot{\hat{\mathbf{\Omega}}}_{\mathrm{P}}.\end{aligned} \tag{39}$$

Using (29)–(34), (39) can be rewritten as

$$\begin{aligned}\dot{V} &= \tfrac{1}{2}\mathbf{e}^{\mathrm{T}}(\mathbf{A}^{\mathrm{T}}\mathbf{P} + \mathbf{P}\mathbf{A})\mathrm{e} + g_n\mathbf{e}^{\mathrm{T}}\mathbf{P}\mathbf{b}(\varepsilon - u_{\mathrm{rc}}) \\ &\quad - g_n\beta_{\mathrm{P}}\hat{\mathbf{\Omega}}_{\mathrm{P}}^{\mathrm{T}}\mathbf{e}^{\mathrm{T}}\mathrm{Pb}\hat{\boldsymbol{\xi}} - g_n\beta_{\mathrm{D}}\hat{\mathbf{\Omega}}_{\mathrm{D}}^{\mathrm{T}}\mathbf{e}^{\mathrm{T}}\mathbf{P}\mathbf{b}\hat{\boldsymbol{\xi}} \\ &\quad + g_n\beta_{\mathrm{D}}\hat{\mathbf{\Omega}}_{\mathrm{P}}^{\mathrm{T}}\dot{\hat{\mathbf{\Omega}}}_{\mathrm{P}} \\ &= \tfrac{1}{2}\mathbf{e}^{\mathrm{T}}(\mathbf{A}^{\mathrm{T}}\mathbf{P} + \mathbf{P}\mathbf{A})\mathrm{e} + g_n\mathbf{e}^{\mathrm{T}}\mathbf{P}\mathbf{b}(\varepsilon - u_{\mathrm{rc}}) \\ &\quad - g_n\beta_{\mathrm{P}}\hat{\mathbf{\Omega}}_{\mathrm{P}}^{\mathrm{T}}\hat{\mathbf{\Omega}}_{\mathrm{P}} - g_n\beta_{\mathrm{D}}\hat{\mathbf{\Omega}}_{\mathrm{D}}^{\mathrm{T}}\hat{\mathbf{\Omega}}_{\mathrm{P}} \\ &= \tfrac{1}{2}\mathbf{e}^{\mathrm{T}}(\mathbf{A}^{\mathrm{T}}\mathbf{P} + \mathbf{P}\mathbf{A})\mathbf{e} + g_n\mathbf{e}^{\mathrm{T}}\mathbf{P}\mathbf{b}(\varepsilon - u_{\mathrm{rc}}) \\ &\quad - g_n\beta_{\mathrm{P}}\hat{\mathbf{\Omega}}_{\mathrm{P}}^{\mathrm{T}}\hat{\mathbf{\Omega}}_{\mathrm{P}}.\end{aligned} \tag{40}$$

Substituting (35) into (40), (40) can be rewritten as

$$\begin{aligned}\dot{V} &= \frac{1}{2}\mathbf{e}^{\mathrm{T}}\left(\mathbf{A}^{\mathrm{T}}\mathbf{P} + \mathbf{P}\mathbf{A} - \frac{1}{\delta}\mathbf{P}\mathbf{b}\mathbf{b}^{\mathrm{T}}\mathbf{P}\right)\mathbf{e} \\ &\quad + g_n\varepsilon\mathbf{b}^{\mathrm{T}}\mathbf{P}\mathbf{e} - g_n\beta_{\mathrm{P}}\hat{\mathbf{\Omega}}_{\mathrm{P}}^{\mathrm{T}}\hat{\mathbf{\Omega}}_{\mathrm{P}} \\ &= \frac{1}{2}\mathbf{e}^{\mathrm{T}}\left(-\mathbf{Q} - \frac{1}{\rho^2}\mathbf{P}\mathbf{b}\mathbf{b}^{\mathrm{T}}\mathbf{P}\right)\mathbf{e} + g_n\varepsilon\mathbf{b}^{\mathrm{T}}\mathbf{P}\mathbf{e} - g_n\beta_{\mathrm{P}}\hat{\mathbf{\Omega}}_{\mathrm{P}}^{\mathrm{T}}\hat{\mathbf{\Omega}}_{\mathrm{P}} \\ &= -\frac{1}{2}\mathbf{e}^{\mathrm{T}}\mathrm{Q}\mathrm{e} - \frac{1}{2}\left(\frac{1}{\rho}\mathbf{b}^{\mathrm{T}}\mathbf{P}\mathbf{e} - g_n\rho\varepsilon\right)^2 + \frac{1}{2}g_n^2\rho^2\varepsilon^2 \\ &\quad - g_n\beta_{\mathrm{P}}\hat{\mathbf{\Omega}}_{\mathrm{P}}^{\mathrm{T}}\hat{\mathbf{\Omega}}_{\mathrm{P}} \\ &\leqslant -\frac{1}{2}\mathrm{e}^{\mathrm{T}}\mathbf{Q}\mathbf{e} + \frac{1}{2}g_n^2\rho^2\varepsilon^2.\end{aligned} \tag{41}$$

Integrating the above inequality (41) yields

$$V(t) - V(0) \leqslant -\frac{1}{2}\int_0^t \mathbf{e}^{\mathrm{T}}\mathbf{Q}\mathbf{e}\,\mathrm{d}t + \frac{g_n^2\rho^2}{2}\int_0^t \varepsilon^2\,\mathrm{d}t. \tag{42}$$

Since $V(t) \geqslant 0$, we obtain the following L^2 criterion

$$\frac{1}{2}\int_0^t \mathbf{e}^{\mathrm{T}}\mathbf{Q}\mathbf{e}\,\mathrm{d}t \leqslant V(0) + \frac{g_n^2\rho^2}{2}\int_0^t \varepsilon^2\,\mathrm{d}t. \tag{43}$$

The knowledge that $\mathbf{Q}$ is a positive definite matrix and the fact $\lambda_{\min}(\mathbf{Q})\mathbf{e}^{\mathrm{T}}\mathbf{e} \leqslant \mathbf{e}^{\mathrm{T}}\mathbf{Q}\mathbf{e}$ imply

$$\int_0^t \mathbf{e}^{\mathrm{T}}\mathbf{e}\,\mathrm{d}t \leqslant \frac{2}{\lambda_{\min}(\mathbf{Q})}V(0) + \frac{g_n^2\rho^2}{\lambda_{\min}(\mathbf{Q})}\int_0^t \varepsilon^2\,\mathrm{d}t. \tag{44}$$

Using Barbalat's lemma, one can see that the tracking error converges to zero in an infinite time. □

Remark 1. The inequality (43) reveals that the integrated squared error of $\mathbf{e}$ is less than or equal to the sum of $V(0)$ and the integrated squared error of ε. Since the $V(0)$ is finite, if ε is squared integrable then we can conclude that $\mathbf{e}$ will approach to zero.

Remark 2. From (44), if the systems starts with the initial condition $V(0) = 0$, i.e., $\mathbf{e}(0) = 0$, $\tilde{\mathbf{v}}(0) = 0$, $\tilde{\mathbf{c}}(0) = 0$, $\tilde{\mathbf{s}}(0) = 0$, $\tilde{\mathbf{\Omega}}_{\mathrm{I}}(0) = 0$, and $\hat{\mathbf{\Omega}}_{\mathrm{P}}(0) = 0$, the L_2 gain must satisfy

$$\sup_{\varepsilon \in L^2[0,t]} \frac{||\mathbf{e}||}{||\varepsilon||} \leqslant \frac{g_n\rho}{\sqrt{\lambda_{\min}(\mathbf{Q})}} \tag{45}$$

where $||\mathbf{e}||^2 = \int_0^t \mathbf{e}^{\mathrm{T}}\mathbf{e}\,\mathrm{d}t$ and $||\varepsilon||^2 = \int_0^t \varepsilon^2\,\mathrm{d}t$. Inequality (45) indicates that when a smaller attenuation level ρ is specified, a better tracking performance can be achieved.

4. Simulation results

In this section, the proposed RITC is applied to control two chaotic dynamic systems to verify its effectiveness. Chaotic systems have been known to exhibit complex dynamical behaviors. Several control techniques have been proposed for the chaotic systems [2,5,8]. It should be emphasized that the development of the RITC does not need to know the dynamics of the controlled system.

Example 1. Consider a second-order chaotic system such as the Duffing's equation describing a special nonlinear circuit or a pendulum moving in a viscous medium [2,5]

$$\ddot{x} = -p\dot{x} - p_1x - p_2x^3 + q\cos(wt) + u = f(\mathbf{x}) + u, \tag{46}$$

where $\mathbf{x} = [x\dot{x}]^{\mathrm{T}}$ is the state vector of the system which is assumed to be available; $f(\mathbf{x}) = -p\dot{x} - p_1x - p_2x^3 + q\cos(wt)$ is the system dynamic function; u is the control effort; and p, p_1, p_2, q and w are real constants. Depending on the choices of these constants, it is known that the solutions of system (46) may display complex phenomena, including various periodic orbits behaviors and some chaotic behaviors [2]. For observing the these complex phenomena, the open-loop system behavior with $u = 0$ was simulated with $p = 0.4$, $p_1 = -1.1$, $p_1 = 1.0$ and $w = 1.8$. The phase plane plots from an initial condition point (0, 0) are shown in Figs. 3(a) and (b) for $q = 2.1$ (chaotic) and $q = 7.0$ (period 1), respectively. The active function of hidden neuron are given with $\mathbf{c} = [-1.0, -0.6, -0.3, 0.0, 0.3, 0.6, 1.0]^{\mathrm{T}}$ and $\mathbf{s} = [0.5, 0.5, 0.5, 0.5, 0.5, 0.5, 0.5]^{\mathrm{T}}$; and the interconnection weights between the input and hidden layers are initiated from ones; and interconnection weights between the hidden and output layers are initiated from zeros. If the learning rates are chosen to be small, then the parameters convergence of the NN will be easily achieved; however, this will result in slow learning speed. On the other hand, if the learning rates are chosen to be large, then the learning speed will be fast; however, the NN may become more unstable for the parameter convergence. The initial settings are chosen through some trials to achieve favorable transient control performance. The control parameters of RITC are selected as $\beta_v = \beta_c = \beta_s = 30$, $\beta_{\mathrm{I}} = 50$, $\beta_{\mathrm{P}} = 5$, $\beta_{\mathrm{D}} = 0.05$, and $\delta = 1.0$. For a choice of $\mathbf{Q} = \mathbf{I}$, $k_1 = 2$ and $k_2 = 1$, solve the Riccati-like Eq. (34), then

$$\mathbf{P} = \begin{bmatrix} 1.5 & 0.5 \\ 0.5 & 0.5 \end{bmatrix}. \tag{47}$$

To compare the tracking efficiency, the RITC with an I-type learning algorithm is applied to control the chaotic system. This is a special case of the developed RITC design method for $\beta_{\mathrm{P}} = 0$ and $\beta_{\mathrm{D}} = 0$. The I-type learning algorithm can be found in most previous research works. The simulation results of the RITC with I-type learning algorithm for $q = 2.1$ and $q = 7.0$ are shown in Figs. 4 and 5, respectively. It is shown that the RITC with I-type learning algorithm can achieve favorable tracking performance. Then, the simulation results of the RITC with PID-type learning algorithm for $q = 2.1$ and $q = 7.0$ are shown in Figs. 6 and 7, respectively. A performance index I is defined as $I = \int e^2\,\mathrm{d}t$. The performance indexes of I-type and PID-type learning algorithm with $q = 2.1$ and 7.0 are shown in Fig. 8. It is shown that the performance index of the proposed PID-type learning algorithm is smaller than that of the I-type learning algorithm. In other words, RITC using the PID-type learning algorithm can achieve better

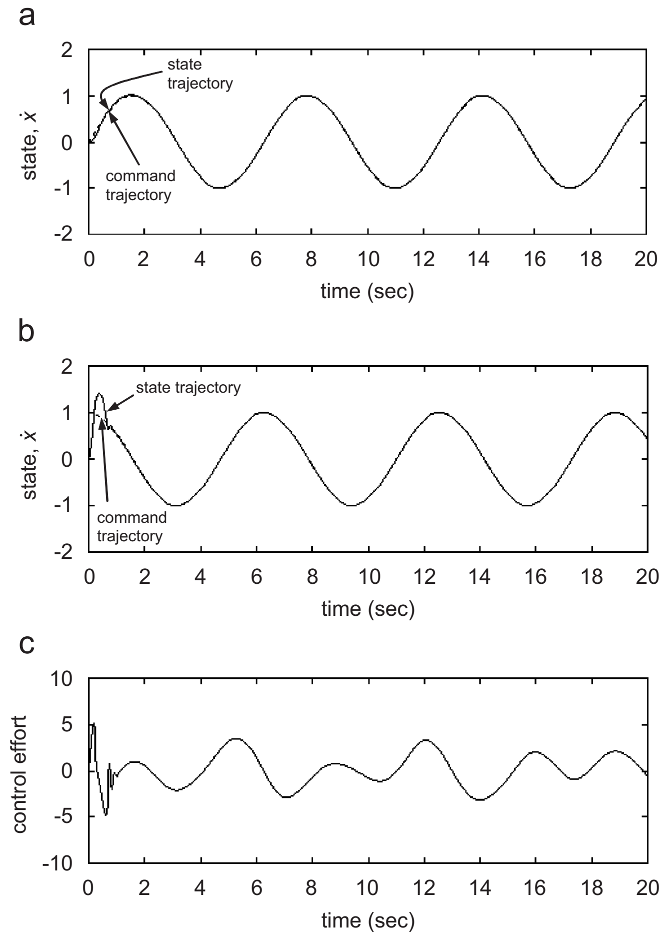

Fig. 4. Simulation results of RITC with the I-type learning algorithm for $q = 2.1$.

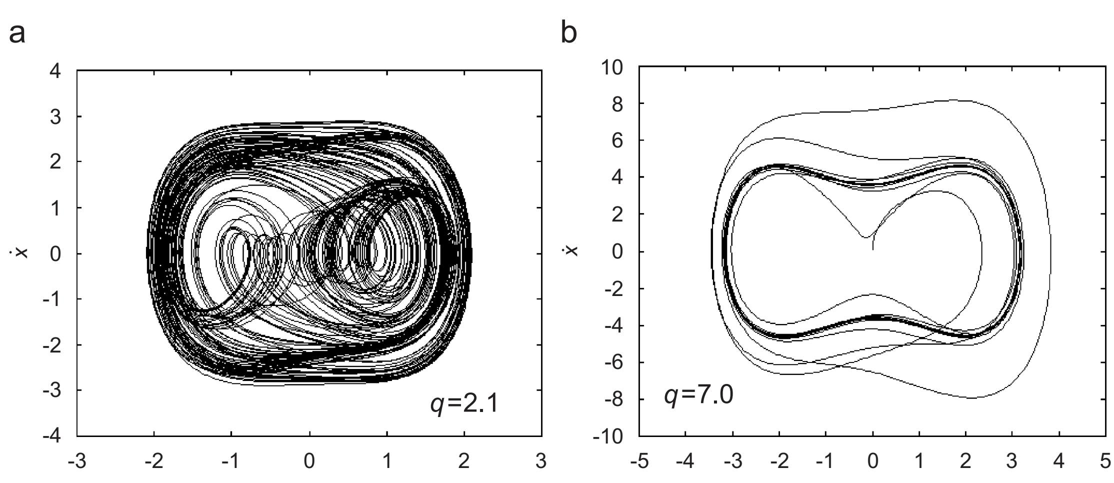

Fig. 3. Phase plane of uncontrolled chaotic system.

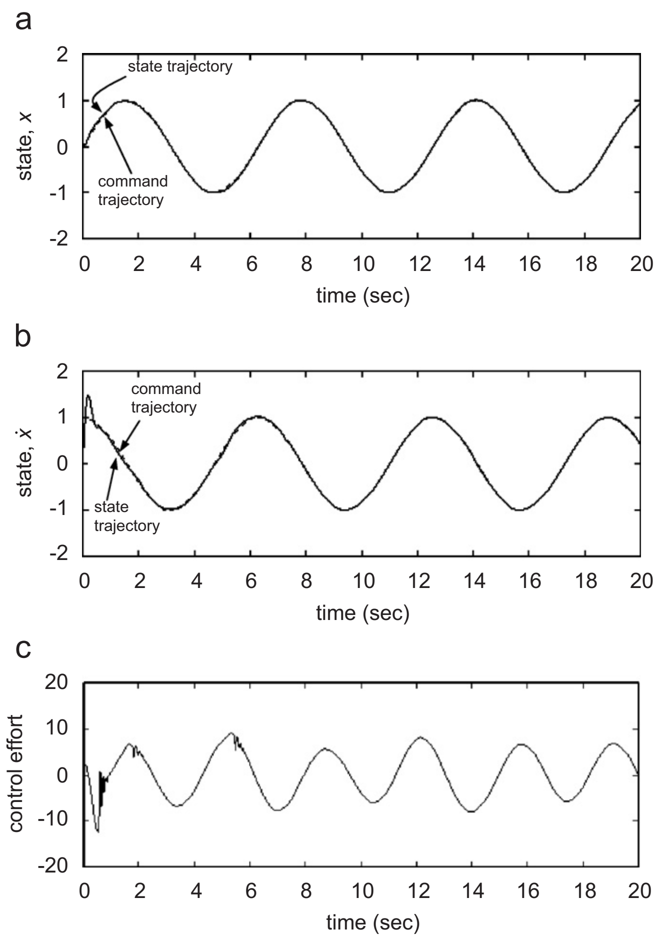

Fig. 5. Simulation results of RITC with the I-type learning algorithm for $q = 7.0$.

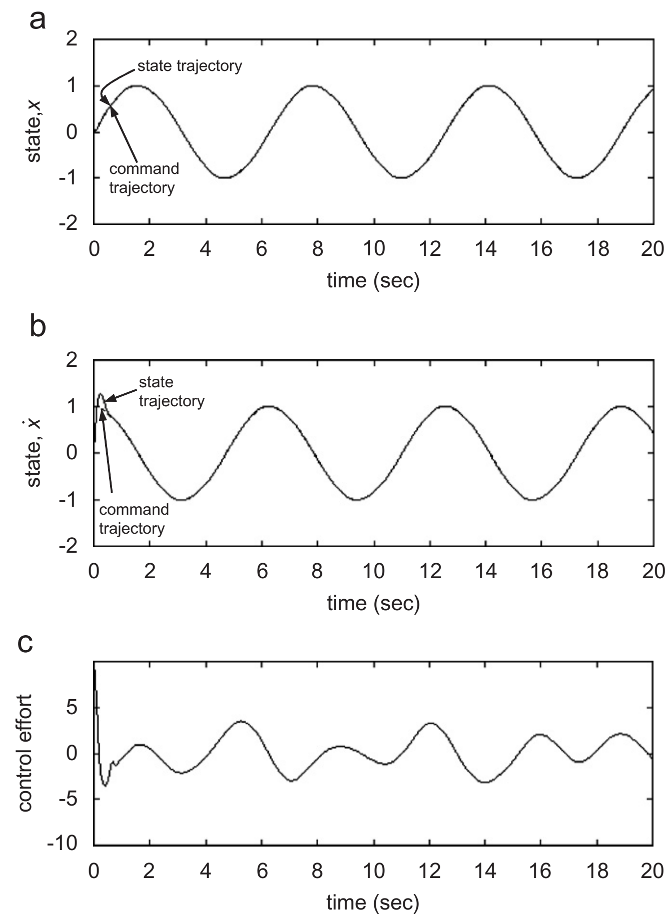

Fig. 6. Simulation results of RITC with the PID-type learning algorithm for $q = 2.1$.

tracking performance than that using I-type learning algorithm.

Example 2. A third-order Chua's chaotic circuit, as shown in Fig. 9, is a simple electronic system that consists of one linear resistor (R), two capacitors (C_1, C_2), one inductor (L), and one nonlinear resistor (λ). It has been shown to own very rich nonlinear dynamics such as chaos and bifurcations. The dynamic equations of Chua's circuit are written as [7]

$$\dot{v}_{C_1} = \frac{1}{C_1}\left(\frac{1}{R}(v_{C_2} - v_{C_1}) - \lambda(v_{C_2})\right),$$
$$\dot{v}_{C_2} = \frac{1}{C_2}\left(\frac{1}{R}(v_{C_1} - v_{C_2}) + i_L\right),$$
$$\dot{i}_L = \frac{1}{L}(-v_{C_1} - R_0 i_L), \tag{48}$$

where the voltages v_{C_1}, v_{C_2} and current i_L are state variables, R_0 is a constant, and λ denotes the nonlinear resistor, which is a function of the voltage across the two terminals of C_1. The λ is defined as a cubic function as

$$\lambda(v_{C_1}) = av_{C_1} + cv_{C_1}^3 \quad (a<0, \quad c>0). \tag{49}$$

The state equations in (48) are not in the standard canonical form. Therefore, a linear transformation is needed to transform them into the form of (20). Then, the dynamic equations of transformed Chua's circuit can be rewritten as

$$\dot{x}_1 = x_2,$$
$$\dot{x}_2 = x_3,$$
$$\dot{x}_3 = f(\mathbf{x}) + u, \tag{50}$$

where $\mathbf{x} = [x_1 x_2 x_3]^{\mathrm{T}}$ is the state vector of the system which is assumed to be available; the system dynamic function

$$f(\mathbf{x}) = \frac{14}{1805}x_1 - \frac{168}{9025}x_2 + \frac{1}{38}x_3 - \frac{2}{45}\left(\frac{28}{361}x_1 + \frac{7}{95}x_2 + x_3\right)^3$$

and u is the control effort. The active function of hidden neuron are given with $\mathbf{c} = [-1.0, -0.6, -0.3, 0.0, 0.3, 0.6, 1.0]^{\mathrm{T}}$ and $\mathbf{s} = [0.5, 0.5, 0.5, 0.5, 0.5, 0.5, 0.5]^{\mathrm{T}}$; and the interconnection weights between the input and hidden layers are initiated from ones; and interconnection weights between the hidden and output layers are initiated from

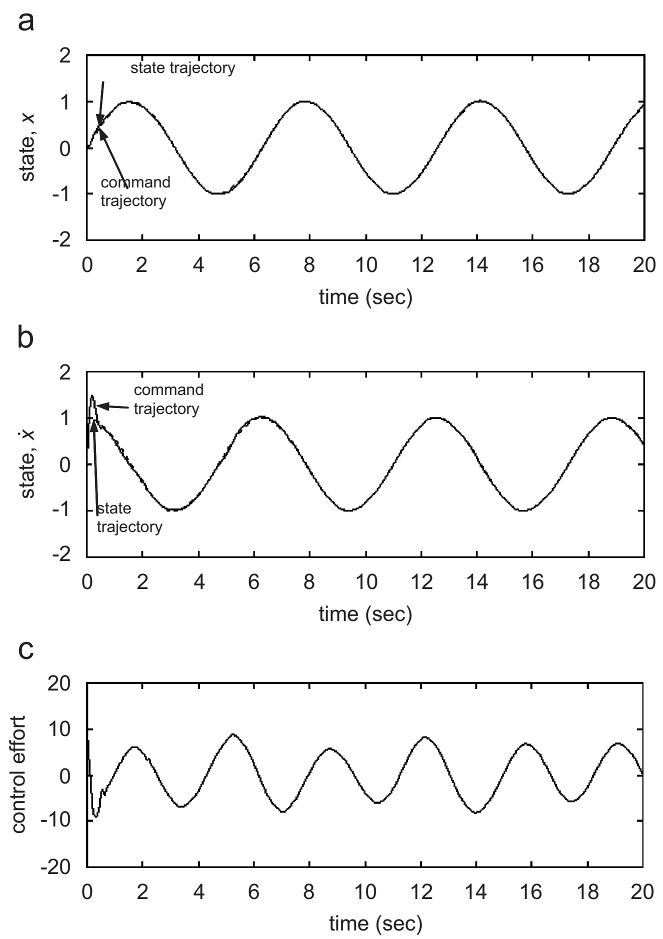

Fig. 7. Simulation results of RITC with the PID-type learning algorithm for $q = 7.0$.

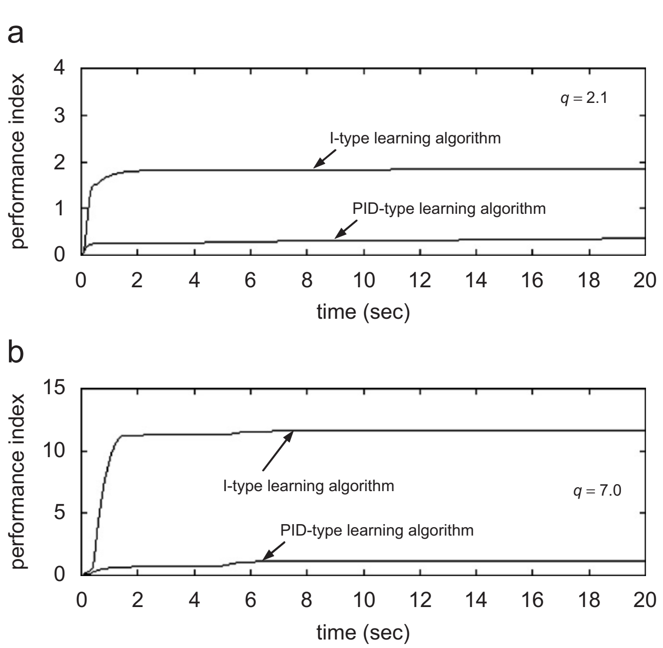

Fig. 8. Performance comparison between I-type and PID-type learning algorithms.

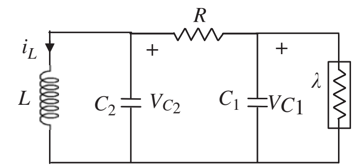

Fig. 9. Chua's chaotic circuit.

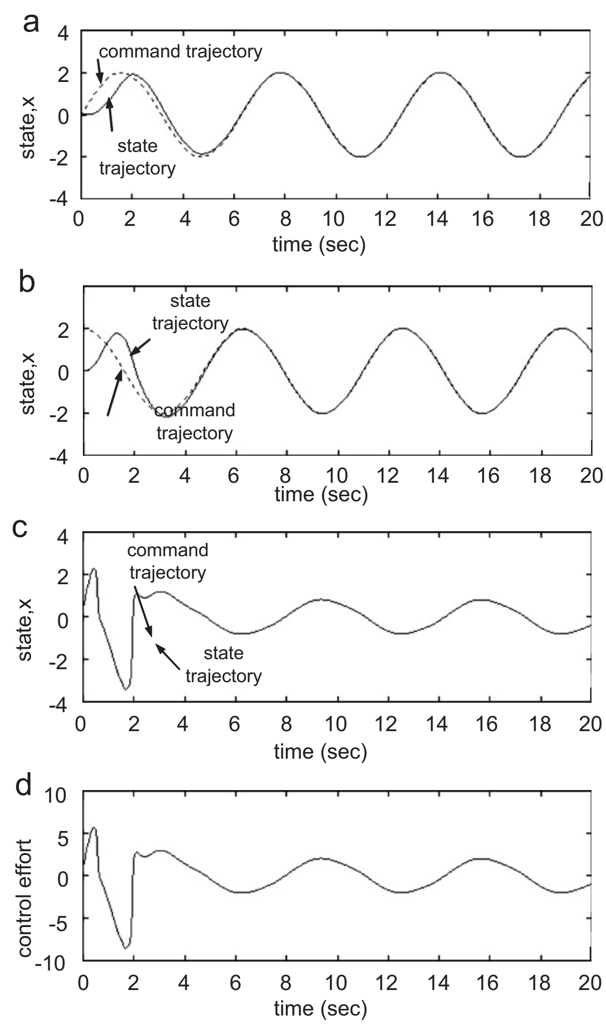

Fig. 10. Simulation results of RITC with $\delta = 1.0$.

zeros. Similar to Example 1, the choice of learning rates will influence the convergent speed of the NN. The initial settings are chosen through some trials to achieve favorable transient control performance. The control parameters are selected as $\beta_v = \beta_c = \beta_s = \beta_{\mathrm{I}} = 10$, $\beta_{\mathrm{P}} = 1$, and $\beta_{\mathrm{D}} = 0.01$. For a choice of $\mathbf{Q} = \mathbf{I}$, $k_1 = 5$, $k_2 = 7$ and $k_3 = 3$, we solve the Riccati-like Eq. (36) and obtain

$$\mathbf{P} = \begin{bmatrix} 1.9323 & 1.2865 & 0.1667 \\ 1.2865 & 2.1667 & 0.2552 \\ 0.1667 & 0.2552 & 0.1510 \end{bmatrix}. \tag{51}$$

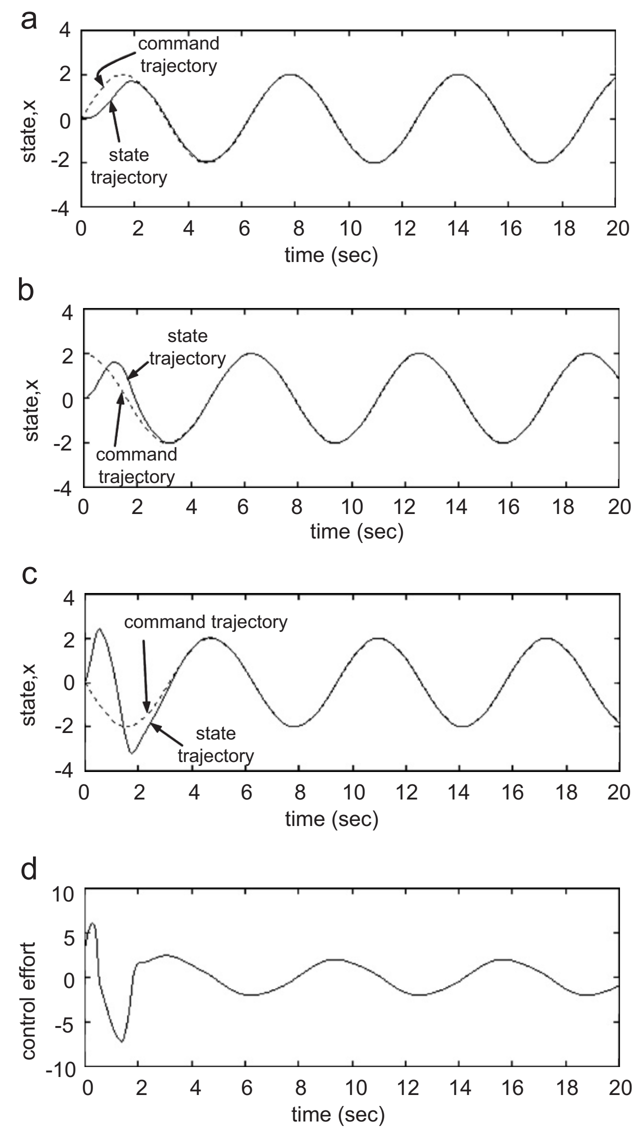

Fig. 11. Simulation results of RITC with $\delta = 0.1$.

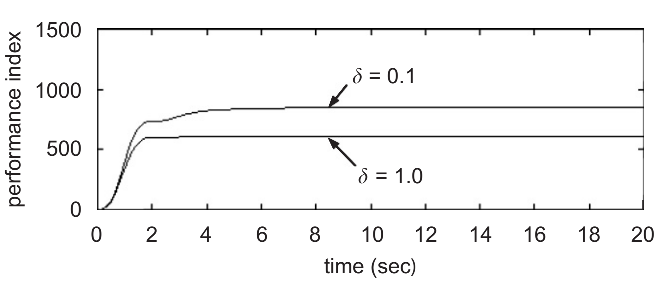

Fig. 12. Performance comparison between $\delta = 1.0$ and 0.1.

The simulation results of the RITC with PID-type learning algorithm for $\delta = 1.0$ and 0.1 and are shown in Figs. 10 and 11, respectively. It can be observed that satisfying tracking performance is achieved for different δ. A performance index I is defined as $I = \int e^2\,dt$. The performance indexes for $\delta = 1.0$ and $\delta = 0.1$ are shown in Fig. 12. It is shown that the performance index for $\delta = 0.1$ is smaller than that for $\delta = 1.0$. In other words, the better tracking performance can be achieved if the specified attenuation level δ is chosen smaller.

5. Conclusions

In this paper, a robust intelligent tracking controller (RITC) for a class of unknown nonlinear systems is proposed. The RITC is comprised of a neural controller and a robust controller. The neural controller is designed to approximate an ideal controller with a PID-type learning algorithm, and the robust controller is designed to achieve L^2 tracking performance with attenuation of disturbances including approximation errors and external uncertainties. Finally, the proposed RITC is applied to control two chaotic dynamic systems to investigate its effectiveness. Simulations verify that favorable tracking performance can be achieved. From the simulation results, three main contributions of this research are concluded: (1) RITC system with PID-learning algorithm can achieve favorable tracking performance in controlling complex nonlinear systems; (2) the convergence of the tracking error and control parameter is accelerated by the PID-type learning algorithm; and (3) an arbitrarily small attenuation level can be achieved if a weighting factor of the robust controller is chosen adequately.

Acknowledgments

The authors are grateful to the associate editor and reviewers for their valuable comments. The authors appreciate the partial financial support from the National Science Council of Republic of China under Grant NSC-93-2218-E-009-053.

References

[1] B.S. Chen, C.H. Lee, H^{∞} tracking design of uncertain nonlinear SISO systems: adaptive fuzzy approach, IEEE Trans. Fuzzy Systems 4 (1) (1996) 32–43.
[2] G. Chen, X. Dong, On feedback control of chaotic continuous-time systems, IEEE Trans. Circuits Systems, I: Fund. Theory Appl. 40 (9) (1993) 591–601.
[3] H. Du, H. Shao, P. Yao, Adaptive neural network control for a class of low-triangular-structured nonlinear systems, IEEE Trans. Neural Network 17 (2) (2006) 509–514.
[4] J.Q. Huang, F.L. Lewis, Neural-network predictive control for nonlinear dynamic systems with time-delay, IEEE Trans. Neural Network 14 (2) (2003) 377–389.
[5] Z.P. Jiang, Advanced feedback control of the chaotic Duffing equation, IEEE Trans. Circuits Systems I 49 (2) (2002) 244–249.
[6] C.K. Lin, Adaptive tracking controller design for robotic systems using Gaussian wavelet networks, IEE Proc. Control Theory Appl. 149 (4) (2002) 316–322.
[7] C.M. Lin, C.F. Hsu, Supervisory recurrent fuzzy neural network control of wing rock for slender delta wings, IEEE Trans. Fuzzy Systems 12 (5) (2004) 733–742.
[8] C.M. Lin, Y.F. Peng, C.F. Hsu, Robust cerebellar model articulation controller design for unknown nonlinear systems, IEEE Trans. Circuits Systems II 51 (7) (2004) 354–358.

[9] O. Omidvar, D.L. Elliott, Neural Systems for Control, Academic Press, New York, 1997.
[10] M.M. Polycarpou, Stable adaptive neural control scheme for nonlinear systems, IEEE Trans. Automatic Control 41 (3) (1996) 447–451.
[11] J.J.E. Slotine, W.P. Li, Applied Nonlinear Control, Prentice-Hall, Englewood Cliffs, NJ, 1991.
[12] R.J. Wai, Development of intelligent position control system using optimal design technique, IEEE Trans. Ind. Electron. 50 (1) (2003) 218–231.
[13] H. Wang, Y. Wang, Neural-network-based fault-tolerant control of unknown nonlinear systems, IEE Proc. Control Theory Appl. 146 (5) (1999) 389–398.
[14] L.X. Wang, Adaptive Fuzzy Systems and Control—Design and Stability Analysis, Prentice-Hall, Englewood Cliffs, NJ, 1994.
[15] W.Y. Wang, M.L. Chan, C.C.J. Chan, T.T. Lee, H^{∞} tracking-based sliding mode control for uncertain nonlinear systems via an adaptive fuzzy-neural approach, IEEE Trans. Systems Man Cybern. Part B 32 (4) (2002) 483–492.

Chun-Fei Hsu (M'05) received his B.S., M.S. and Ph.D. degrees in Electrical Engineering from the Yuan-Ze University, Taiwan, Republic of China in 1997, 1999 and 2002, respectively. After graduation, he joined the Department of Electrical and Control Engineering, National Chiao-Tung University, Taiwan, Republic of China. During 2002–2006, he was doing a post-doctor with Professor Tsu-Tian Lee about virtual-reality dynamic simulator and intelligent transportation system. His research interests include servomotor drives, adaptive control, flight control and intelligent control using fuzzy system and neural network technologies.

Guan-Ming Chen was born in Kaohsiung, Taiwan, ROC in 1975. He received his B.S. degree in Electrical and Control Engineering from the Chiao Tung University, Hsinchu, Taiwan in 1999 and M.S. degree in Electronic Engineering from the Fu-Jen Catholic University, Taipei, Taiwan in 2003. Since September 2003, he has been pursuing his Ph.D. degree in the Department of Electrical and Control Engineering at the Chiao Tung University, Taiwan. His research interests include neural network, fuzzy logic system, adaptive control, and intelligent control.

Tsu-Tian Lee (M'87–SM'89–F'97) was born in Taipei, Taiwan, ROC, in 1949. He received his B.S. degree in Control Engineering from the National Chiao-Tung University (NCTU), Hsinchu, Taiwan, in 1970, and M.S., and Ph.D. degrees in Electrical Engineering from the University of Oklahoma, Norman, in 1972 and 1975, respectively. In 1975, he was appointed Associate Professor and in 1978 Professor and Chairman of the Department of Control Engineering at the NCTU. In 1981, he became Professor and Director of the Institute of Control Engineering, NCTU. In 1986, he was a Visiting Professor and in 1987, a Full Professor of Electrical Engineering at the University of Kentucky, Lexington. In 1990, he was a Professor and Chairman of the Department of Electrical Engineering, National Taiwan University of Science and Technology (NTUST). In 1998, he became the Professor and Dean of the Office of Research and Development, NTUST. Since 2000, he has been with the Department of Electrical and Control Engineering, NCTU, where he is now a Chair Professor. Since 2004, he has been with the National Taipei University of Technology (NTUT), where he is now President. Prof. Lee received the Distinguished Research Award from the National Science Council, ROC, in 1991–1998, and the Academic Achievement Award in Engineering and Applied Science from the Ministry of Education, ROC, in 1997, the National Endow Chair from the Ministry of Education, ROC, in 2003, and the TECO Science and Technology Award from TECO Technology Foundation in 2003. He was elected to the grade of IEE Fellow in 2000, respectively. He became a Fellow of New York Academy of Sciences (NYAS) in 2002. He has served as Member of Technical Program Committee and Member of Advisory Committee for many IEEE sponsored international conferences. He is now the Vice President of Membership, a member of the Board of Governors, and the Newsletter Editor for the IEEE Systems, Man, and Cybernetics Society.